While our power spectrum is not as broad as those in the toroidal experiments with weak shear, the spectrum in the simulation is measured in a transient state from initial linear phase to the final turbulent state while the laboratory experiments measure fully developed steady-state turbulence driven externally. Furthermore, the spectrum in the laboratory experiments is averaged over different $k_{\|}$ modes and the plasma radius. The simulation spectrum will be monotonic if such averaging is carried out.

We have simulated the same example, keeping 11 modes in z ($n = 0, \pm 1, \ldots, \pm 5$), and found the results essentially the same. We have also included a magnetic shear in the simulations and found the convective cells to persist for $L_s/L_n \lesssim 25$. The details will be reported later.[8]

We acknowledge useful discussions with Dr. W. W. Lee, Dr. V. Arunasalum, and Dr. M. Okabayashi.

*Work supported by the U. S. Energy Research and Development Administration under Contract No. E(11-1)-3073.

[1]C. Z. Cheng and H. Okuda, to be published, and Princeton Plasma Physics Laboratory Report No. PPPL-1204, 1976 (unpublished).

[2]E. Mazzucato, Phys. Rev. Lett. 36, 792 (1976).

[3]S. M. Hamberger, L. E. Sharp, J. B. Lister, and S. Mrowka, Phys. Rev. Lett. 37, 1345 (1976).

[4]M. Okabayaski and V. Arunasalum, Princeton Plasma Physics Laboratory Report No. PPPL-1310, 1976 (unpublished).

[5]M. W. Alcock, D. E. T. F. Ashby, J. G. Gordey, T. Edlington, W. H. W. Fletcher, E. M. James, J. Malmberg, A. C. Riviere, D. F. H. Start, and D. R. Sweetman, in Proceedings of the Sixth Internatioanl Conference on Plasma Physics and Controlled Fusion, Berchtesgaden, West Germany, 6–13 October, 1976 (International Atomic Energy Agency, Vienna, to be published).

[6]W. W. Lee and H. Okuda, Phys. Rev. Lett. 12, 870 (1976).

[7]H. Okuda and J. M. Dawson, Phys. Fluids 16, 408 (1973).

[8]H. Okuda and C. Z. Cheng, Princeton Plasma Physics Laboratory Report No. PPPL-1328 (to be published).

[9]J. Canosa, J. Krommes, C. Oberman, H. Okuda, K. Tsang, J. M. Dawson, and T. Kamimura, in *Proceedings of the Fifth International Conference on Plasma Physics and Controlled Nuclear Fusion Research, Tokyo, Japan, 1974* (International, Atomic Energy Agency, Vienna, Austria, 1975), p. 177.

[10]J. B. Drake, J. R. Greenwood, G. A. Navratil, and R. S. Post, Phys. Fluids 20, 148 (1977).

Chain-Pairing Effects in One-Dimensional Conjugated Polymers and Semiconductors

G. P. Agrawal, C. Cojan, and C. Flytzanis
Laboratoire d'Optique Quantique, Ecole Polytechnique, 91128 Palaiseau, France*
(Received 20 December 1976)

We explain the absorption line and resonant Raman lines splittings together with the selection rules at low temperatures in polydiacetylene polymer crystals in terms of a chain-pairing mechanism arising from side-group interactions between the conjugated carbon chains. The symmetry of the pairing configuration has drastic effects on the one- and two-photon absorption spectra.

The availability of large defect-free crystals on the solid-state polymerization[1] of diacetylene monomers $R-C\equiv C-C\equiv C-R$, R being a radical, has triggered a growing interest in this new class of materials. Large separation among the chains and bond alternation along the conjugated carbon chains[2] confer to these materials an isolator-type behavior across the chains but a semiconducting one along the chain direction. This is reflected[3] in an intense and relatively narrow absorption peak around 2 eV at room temperature arising from π-electron transitions.

It has recently been established[4,5] that at lower temperatures, below 160°K for the polydiacetylent-*bis* toluene sulphonate (PTS diacetylene, $R=CH_2-O-SO_2-\Phi-CH_3$), the peak splits into two narrow and equally intense lines, the separation between them increasing with decreasing temperature and reaching a value $\simeq 500$ cm^{-1} at 4°K for the PTS-diacetylene. Such a remarkable behavior is also observed[6] in the resonant Raman scattering (RRS) spectra. Furthermore, around the same temperature the system probably undergoes[7] a phase transition doubling the unit-cell dimensions along the crystallographic a axis (the b axis is the chain direction). It has been verified that these splittings are not due to the appearance of two different chains per unit cell and

that the two components have the same polarization (no Davydov splitting).

In this Letter, we show that these observations can be well explained by admitting that the polymer chains, which can be assumed to be independent at room temperature, *get coupled in pairs* below a certain critical temperature T_c in such a way that *the π electrons may leak from one chain over to its partner chain;* the pairs are assumed to be independent. This chain pairing most likely results from a rearrangement of the side groups R which, for the neighboring chains, strongly overlap. The conclusions drawn below are insensitive to the details of the pairing mechanism as long as one occurs and provides a leakage of the π electrons between the two pairing chains —they rely on the one-dimensionality of the system, a consequence of the large delocalization of the π electrons in one direction only. As inferred from Raman[8] and x-ray studies, bond alternation is very strong in these systems and, therefore, we only need to restrict ourselves to the one-electron tight-binding description; electron correlation[9] is thus not included.

At temperatures $T>T_c$, the absorption peak at 2 eV and the other linear and nonlinear optical properties are then due to valence- to conduction-band transitions of π electrons in independent and infinitely long chains.[9,10] The π-band energies $\epsilon_n(k)$ and wave functions $\psi_{nk}(x)=e^{ikx}u_{nk}(x)$ were obtained[10,11] and used to evaluate[10,11] the dipole-transition matrix elements[11] $\Omega_{nn'}(k)=(2a)^{-1}\int u_{nk}^{*}\times(\partial u_{n'k}/\partial k)dx$, where $2a$ is the length of the unit cell (u.c.) along a single carbon chain. With use of existing values[11] for the intrachain hopping energies β_1, β_2, and β_3 for the single, double, and triple bonds, respectively [see Fig. 1(a)], such a band picture properly accounts[10,11] for all observed properties at room temperature and for the single narrow absorption line at 2 eV, in particular. This is because the dipole-transition strength from valence to conduction band, Ω_{vc}, rises rapidly as we approach the Brillouin zone (BZ) edge, attaining its maximum value there, where the joint density of states is infinite, a characteristic feature of an one-dimensional system.[10] Because of these features, we can greatly simplify the algebra without affecting the physical contents by replacing the polydiacetylene chain with an optically equivalent polyene (dimerized) chain which reproduces the essential BZ-edge details; we shall do so in the following. The intrachain hopping energies $\tilde{\beta}_1$ and $\tilde{\beta}_2$ of the polyene chain are obtained from those of the polydiacetylene chain, β_i, by requiring that the band gaps occurring at the center and edge of the BZ are identical for the two types of chains.

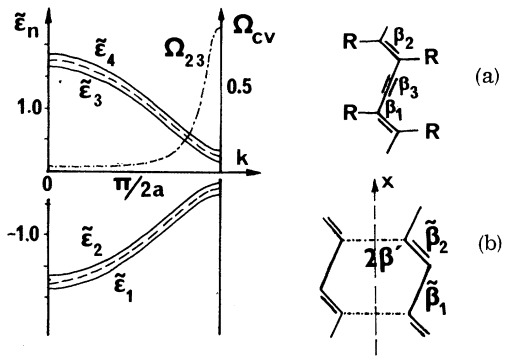

FIG. 1. Band energies (in units of $\tilde{\beta}_2$) and $\Omega_{23}=\Omega_{14}$ (in units of a) at $T<T_c$ for a pair of coupled associated polyene chains ($\tilde{\beta}_1/\tilde{\beta}_2=0.75$, $4\beta'/\tilde{\beta}_2=0.014$ eV and $\tilde{\beta}_2=4.0$ eV); subscripts 1 and 2 refer to the valence bands (v), and 3 and 4 to the conduction ones (c). The bands for individual chains ($T<T_c$, zero coupling) are also shown (dashed bands). (a) Individual polydiacetylene chain; (b) S-pairing configuration.

At low temperatures, $T<T_c$, the chains are coupled in pairs and the π electrons of a chain may hop over to its partner chain; this π-electron leakage will be taken into account by introducing an interchain hopping energy $2\beta'$ [see Fig. 1(b)]. It will be a function of the temperature, vanishing for $T>T_c$; its actual dependence on T will reflect the origin of the pairing, but we shall not be concerned with it presently. *The chain pairs are assumed to be independent so that the one-dimensional character of the system is preserved.*

On pairing of two infinite dimerized chains, we find that there are two possible configurations depending on whether the even sites of one chain are coupled to the odd or the even sites of its partner chain. In the former case the pair has an inversion symmetry (S configuration) and belongs to the point group C_{2h}, while in the other case the pair has reflection symmetry but no center of inversion (A configuration) and belongs to the point group C_{2v}; the configuration plane is assumed to coincide with the x-y plane, and the principal axis is the z axis. The two configurations possess the same band structure with

$$\epsilon_n=\pm\tilde{\beta}_2[(1+\delta^2+\nu^2+2\nu\cos\theta)^{1/2}\pm\delta]=\tilde{\beta}_2\zeta_n, \qquad (1)$$

when $n=1$ to 4 in order of increasing energy (Fig. 1), $\nu=\tilde{\beta}_1/\tilde{\beta}_2$, $\delta=\beta'/\tilde{\beta}_2$ and $\theta=ka$, but strikingly different wave functions ψ_{nk} and dipole-transition matrix elements $\Omega_{nn'}$, hence different absorption

spectra.

In the S-pairing configuration we obtain

$$\psi_{nk}=\frac{C_n}{\sqrt{2N}}\sum_{r=1}^{N} e^{ir\theta}\left[\left(\varphi_{2r}'+\frac{\xi_0}{\xi_n}e^{in}\varphi_{2r+1}'\right)\right.$$

$$\left.\pm e^{-i\eta}\left(\frac{\xi_0}{\xi_n}\varphi_{2r}''+e^{i\eta}\varphi_{2r+1}''\right)\right], \quad (2)$$

$$\Omega_{13}=\Omega_{24}=a\nu\delta\sin\theta/2\xi_0(\xi_0^2+\delta^2), \quad (3)$$

$$\Omega_{14}=\Omega_{23}=ia(1-\nu^2)/4\xi_0^2, \quad (4)$$

where $\xi_0=(1+\nu^2+2\nu\cos\theta)^{1/2}$, $\exp(i\eta)=(\nu+e^{i\theta})/(\nu+e^{-i\theta})$, and $C_n=\xi_n/(\xi_0^2+\xi_n^2)^{1/2}$; φ_m' and φ_m'' are the atomic orbitals on the two chains of the pair. For $\beta'=0$, Eqs. (1)–(4) reduce to those of a single bond-alternated (dimerized) chain.[11]

Although in general all transitions are allowed, near the BZ edge ($\theta\leq\pi$) the transitions $1\rightarrow 3$ and $2\rightarrow 4$ are almost forbidden there [Eq. (3)]. Consequently, the one-photon absorption spectrum will consist of two narrow peaks corresponding to the transitions $2\rightarrow 3$ and $1\rightarrow 4$, separated by $4\beta'$ [Eq. (1)]. In Fig. 2 we have plotted the absorption spectrum; it shows a striking resemblance with the one observed by Reimer *et al.*[5] and by Bloor, Preston, and Ando[4] indicating that in polydiacetylene polymers at low temperatures ($T<160$°K) the S configuration is preferred[12] on pairing. Moreover, the two peaks show the same polarization, in agreement with the experiment. At 4°K the measured splitting reaches 0.062 eV and corresponds to $\beta'\simeq 0.015$ eV, which is 0.5% of the intrachain hopping energies; it is remarkable that such a weak short-range coupling leads to such well-observed effects.

The S-pairing configuration of chains also leads to selection rules for the RRS which explain the results of Batchelder and Bloor.[6] It was observed that below T_c each of the Raman components of a split line shows selective enhancement, the lower-frequency component being coupled to the high-frequency absorption peak and vice versa. It is clear that on pairing, when the degeneracy of the coupled system is lifted, each vibrational level of the initially independent chains will split into two, in complete analogy with the electronic level splitting; *accordingly, each vibronic level (valence electronic level + vibration) of the individual chains (at $T>T_c$) will split into four vibronic levels (two doublets) at $T<T_c$* (see Fig. 3).

For the RRS the scattering cross section is $\sigma\sim K^2$ where the transition strength K is given by

$$K=\sum_i \frac{M_{gi}M_{if}}{\hbar(\omega_0-\omega_{ig})}, \quad (5)$$

where the subscripts g, f, and i refer, respectively, to the ground (valence) electronic state, final vibronic state, and the involved (conduction) intermediate state of energy $\hbar\omega_{ig}$; ω_0 and ω_s are the incident pump and scattered Stokes frequencies, respectively. M_{gi} and M_{if} are related to the dipole-transition matrix elements $\Omega_{nn'}$ given by Eqs. (3) and (4); they are nonzero only when the two involved states are of opposite parity. Al-

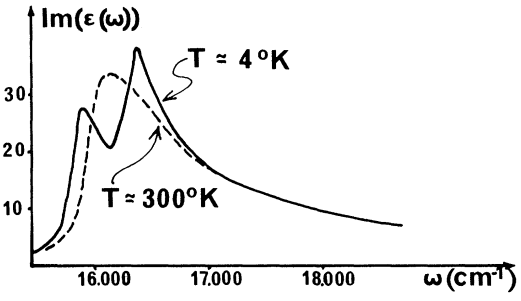

FIG. 2. Calculated one-photon absorption spectrum [imaginary part of the dielectric constant $\epsilon(\omega)$] at 4°K of chain pairs in the S configuration; for comparison, the room-temperature spectrum is also shown.

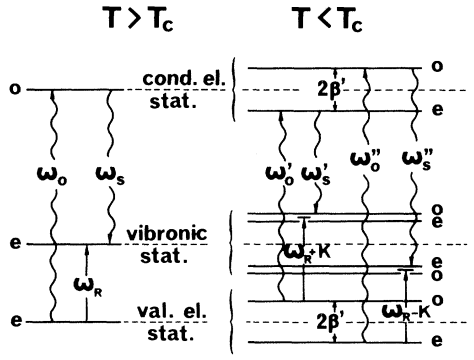

FIG. 3. Allowed optical transition scheme at low and high temperatures for the resonant Raman scattering; ω_0, ω_0', and ω_0'' are pump frequencies and ω_s, ω_s', and ω_s'' the corresponding scattered frequencies and ω_R is the frequency of a Raman-active mode at $T>T_c$. All the energy levels correspond to the BZ edge (Fig. 1). The letters e and o stand for even and odd parity attributed to the states. The position and parity assignment of the four vibronic levels (two doublets) at $T<T_c$ was obtained by diagonalizing a 4×4 matrix; κ measures the vibration-induced change of the π-electron interchain energy β'. One can easily see that the nonresonant Raman spectrum at $T<T_c$ will show two lines 2κ apart ($\kappa=2$ cm^{-1}).

though no definite parity can be assigned to the band states of arbitrary k, [Eq. (2)], *for the S configuration belonging to the point group* C_{2h}, the one we are interested in, *the states are of definite parity at the edge of the BZ,* where the transitions essentially take place; as already discussed in connection with the absorption-peak splitting, this amounts to making the transitions $1 \rightarrow 3$ and $2 \rightarrow 4$ symmetry-forbidden.

In Fig. 3 we have shown the transition scheme for the RRS below and above T_c with this simple rule in mind: Only the two cases when $\hbar\omega_0$ is in resonance with the allowed electronic transitions $2 \rightarrow 3$ and $1 \rightarrow 4$ are shown (ω_0' and ω_0'', respectively). Use was made of the fact that, upon coupling, each level is split into two levels of definite parity. This can be clearly seen for the electronic wave functions [cf. Eq. (2)]; a similar behavior is found for the vibronic states.[13] Thus S-pairing configuration fully accounts for the RRS results as well as for the nonresonant Raman spectrum. If no such selection rules were operative, a much more complicated structure would be obtained.

On pairing, the electron delocalization changes,[10] and this may have striking effects on the nonlinear optical properties, still unobserved; extraordinary high values of the third-order susceptibility have been measured[14] in PTS-diacetylene at room temperature, which is indicative of the π-electron delocalization. Finally, the two-photon absorption spectrum shows some marked changes on crossing T_c. The selection rules and the intensity of the two-photon transitions are determined[15] by $\nabla_k(\Omega_{cv}/\omega_{cv})$. For $2 \rightarrow 3$ and $1 \rightarrow 4$ they are forbidden at the BZ edge ($k = \pi/a$), where the one-photon transitions mostly occur, and give rise to the two-peak structure in the S configuration (Figs. 1 and 2). On the other hand, $2 \rightarrow 4$ (and $1 \rightarrow 3$) is now allowed there (while it is forbidden by one-photon transitions); its strength, however, is only β'^2, the square of the interchain π-electron hopping energy, and the corresponding peak may be barely observable since it overlaps with the two-photon transitions $2 \rightarrow 3$ for $k < \pi/a$ (they are allowed there).

In polymer crystals with one chain per unit cell, it is evident that such a pairing as adopted in the present model will result in a phase transition at T_c, doubling the unit-cell dimension in a direction across the chains. We should, however, remark that in certain polydiacetylene polymer crystals and in the PTS-diacetylene in particular, the crystal structure stabilizes[2] with two chains per unit cell along the c direction, the direction of maximum overlap of the side groups. If the coupling below T_c occurs in this direction no phase transition can result, while with the coupling along the a direction a transition necessarily follows. Although the former seems more favorable, on account of the shortest interchain distance, the latter cannot be ruled out because of the strong stereochemical selectivity of some side-group interactions.

In conclusion, we have shown in terms of a simple but quite general model that the low-temperature behavior of the polydiacetylene polymer crystals can be well explained by assuming a chain-pairing scheme. We stress the fact that this pairing preserves the one-dimensionality of the system.

We acknowledge fruitful discussions with J. Ducuing, D. Bloor, R. H. Baughman, and R. Pick.

---

*Laboratoire propre du Centre National de la Recherche Scientifique.

[1]G. Wegner, Makromol. Chem. 145, 85 (1971).

[2]D. Kobelt and F. Paulus, Acta Crystallogr., Sect. B 30, 231 (1974); R. H. Baughman, J. D. Witt, and K. C. Yee, J. Chem. Phys. 60, 4755 (1974).

[3]D. Bloor, D. J. Ando, F. H. Preston, and G. C. Stevens, Chem. Phys. Lett. 24, 407 (1974).

[4]D. Bloor, F. H. Preston, and D. J. Ando, Chem. Phys. Lett. 38, 33 (1976).

[5]B. Reimer, H. Baessler, J. Hasse, and G. Weiser, Phys. Status Solidi (b) 73, 709 (1976).

[6]D. N. Batchelder and D. Bloor, Chem. Phys. Lett. 38, 37 (1976).

[7]D. Bloor, private communication.

[8]An alternative description of the semiconducting state in independent polyene chains including electron correlation is given in A. A. Orchinnikov, I. I. Ukrainskii, and G. V. Kventsel, Usp. Fiz. Nauk 108, 81 (1972) [Sov. Phys. Usp. 15, 575 (1973)]. Within the Hartree-Fock approximation, chain-pairing effects can be included there too along the lines discussed below, but with considerable computational effort.

[9]E. G. Wilson, J. Phys. C 8, 727 (1975).

[10]C. Cojan, G. P. Agrawal, and C. Flytzanis, Phys. Rev. B 15, 909 (1977).

[11]G. P. Agrawal and C. Flytzanis, Chem. Phys. Lett. 44, 366 (1976).

[12]In the A configuration on the other hand, one finds $\Omega_{23} = \Omega_{14} = 0$ but $\Omega_{13} = \Omega_{24} \neq 0$ and thus no splitting occurs.

[13]Thus at the edge of the Brillouin zone, one has the eight-level scheme shown in Fig. 3: Two valence electronic states $\psi_V^{\pm} = (\psi_{V'} \pm \psi_{V''})/\sqrt{2}$ [Eq. (2)], two conduction electronic states $\psi_C^{\pm} = (\psi_{C'} \pm \psi_{C''})/\sqrt{2}$ [Eq. (2)], and four vibronic levels $\psi_V^{\pm}\chi^{\pm}(Q)$ for each Raman-active mode Q of the individual chains. All states have definite parity [+ stands for even (e) and − for odd (o) parities] and their positions are obtained by diagonalizing

the appropriate coupling Hamiltonian.
[14]C. Sauteret, J.-P. Hermann, R. Frey, F. Pradère, J. Ducuing, R. R. Chance, and R. H. Baughman, Phys. Rev. Lett. 36, 956 (1976).
[15]P. M. Mednis, Fiz. Tverd. Tela 14, 2531 (1972) [Sov. Phys. Solid State 14, 2195 (1973)].

New Phase Transition Observed at 46 K in Tetrathiafulvalene-Tetracyanoquinodimethane (TTF-TCNQ)

D. Djurek, K. Franulović, M. Prester, and S. Tomić
Institute of Physics, University of Zagreb, Zagreb, Yugoslavia

and

L. Giral and J. M. Fabre
Laboratoire de Chimie Organique Structurale, Université des Sciences et Techniques du Languedoc, Montpellier, France

(Received 16 November 1976; revised manuscript received 15 February 1977)

We have measured the heat capacity of TTF-TCNQ in the vicinity of the low-temperature transitions. High-resolution measurements, realized by the improvement of standard relaxation techniques, lead to the observation of four phase transitions at 52.6, ~ 49–48, 46, and 37 K. The new transition observed at 46 K is tentatively attributed to the softening of $0.59b^*$ mode in TTF-TCNQ.

X-ray[1] and neutron[2] scattering studies of TTF-TCNQ have revealed an interesting sequence of structural phase transitions in the temperature range around 50 K. The precusor effect to these anomalies are the one-dimensional diffuse scatterings at $0.295b^*$ $2k_F$ mode and $0.59b^*$ $4k_F$ mode, where b^* is the reciprocal-chain axis. The usual interpretations[3-5] of the low-temperature phase transitions involve only the deformation components of two sets of chains around $0.295b^*$. This is qualitatively correct if $0.59b^*$ scattering is either completely independent or the secondary (harmonic) or induced[5] effect. In the low-temperature range (below 20 K), this latter scattering occurs at positions[1,2] which are just the double of those corresponding to the scattering at $0.295b^*$. This suggests the "harmonic" interpretation. However, at high temperatures the scattering at $0.59b^*$ moves to $0.55b^*$, and is the only one detected. Thus, it might be thought[3] of as being an effect roughly independent of that at $0.295b^*$.

While the conductivity measurements revealed anomalies at 53[6] and 38 K,[7] measurement of magnetic susceptibility,[8] as well as specific heat,[9] do not indicate the presence of the additional transitions to the 53 K transition. For obvious reasons, the specific heat measurement is, beside x-ray or neutron experiments, well suited for resolving this question. However, measurements of specific heat anomalies related to the low-temperature phase transitions in TTF-TCNQ represent a serious challenge to calorimetric methods partly because the samples are available in the form of small prolate platelets weighing up to 50 μg with an appreciably smaller thermal conductivity than that of metals. Calorimetric techniques (ac techniques and heat-pulse techniques) of the relaxation type are least suited when small samples are involved. After a heat pulse is brought to the sample, it begins to fall off as a result of heat flowing to the sink through the connecting leads. The important condition for the use of a relaxation technique is that the intrinsic relaxation time of the specimen τ_{int} is negligible by comparison to the specimen-sink relaxation time τ_{ss}; that is,

$$\tau_{int} \ll \tau_{ss} = r_t c_{sp},$$

where r_t and c_{sp} are thermal resistance to the sink and specimen heat capacity, respectively. In many cases, attention must be paid to the sample thermal resistance and to the heat capacity of the connecting leads. In the case when the heat capacity (c_L) or the thermal resistance of the connecting leads (r_t) are comparable to those of the specimen (labeled as r_{int} and c_{sp}), the empirical formula[10] for the effective time constant of the specimen temperature relaxation is obtained in the form

$$\tau_{eff} = (r_t + \alpha r_{int})[c_L + (2-\epsilon)\beta^{-1} c_{sp}], \quad (1)$$

where $\epsilon = (c_L - c_{sp})/c_{sp}$, $c_L \geq c_{sp}$, $\beta \geq 4$, and $0 < \alpha < 1$ according to the geometry chosen. The effective relaxation time is remarkably insensitive to